Patient CT and MRI Findings

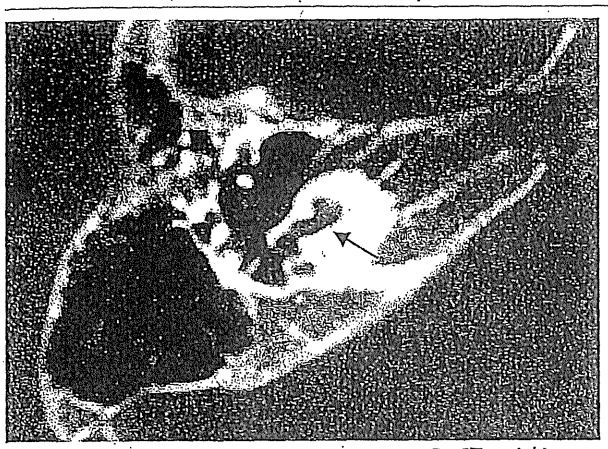

1R. CT: axial image

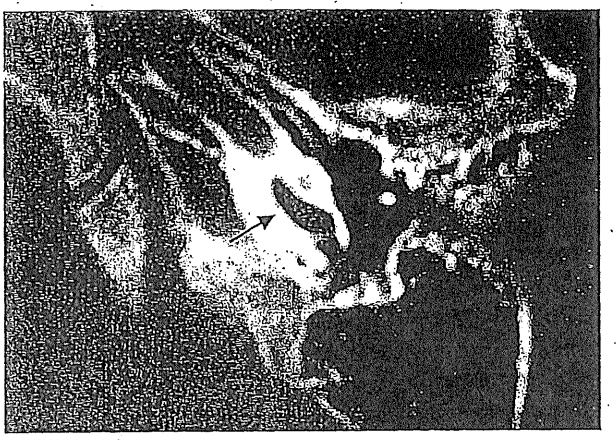

1L. CT: axial image

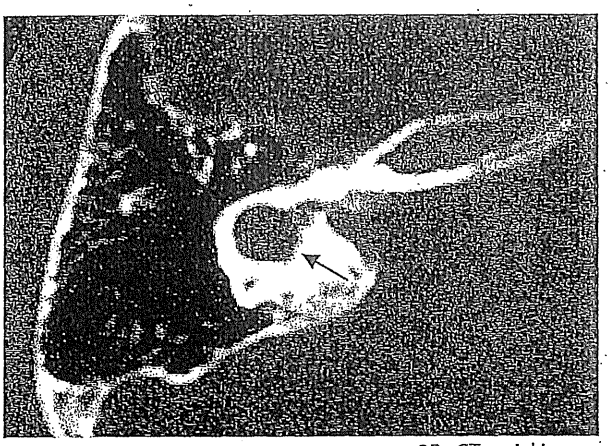

2R. CT: axial image

2L. CT: axial image

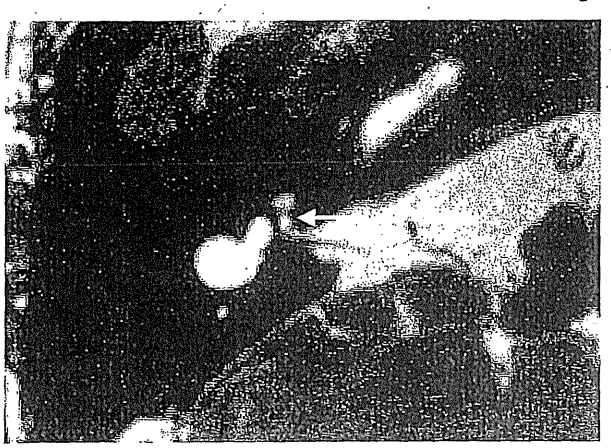

3R. MRI: axial image

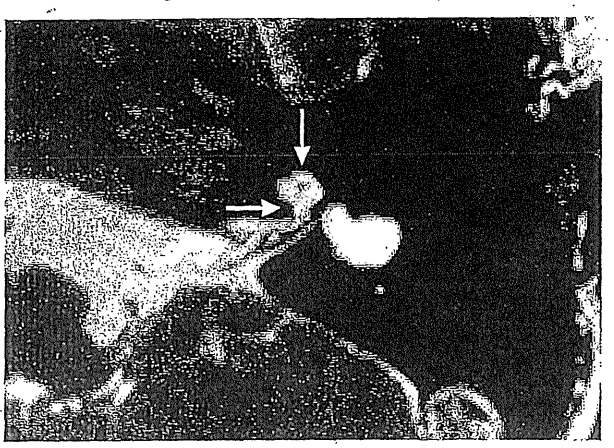

3L. MRI: axial image

Fig. 36. (Case 6) CT and MRI

[Patient CT and MRI Findings]

On the right side, the basal turn and upper turn of the cochlea are unseparated and cystic (1R: ↖). The lateral semicircular canal is also cystic (2R: ↖), with the vertical semicircular canal existing separately from this cystic vestibule. The right inner ear is an incomplete partition type I according to the Sennaroglu-Saatci classification. On the MRI a partition is faintly visible between the inner ear and the internal auditory canal (3R: ⇦).

Meanwhile, on the left side, the basal turn of the cochlea is thicker than normal, and the second turn and beyond is cystic. The vestibule and lateral semicircular canal form a single cyst (2L: ↗), but the vertical semicircular canal is separate from it. The left ear is also diagnosed as an incomplete partition type I. On the left side, no partition is visible between the internal auditory canal and the cochlea (3L: ⇨). In the MR images of the cochlea, a hypointense area corresponding to the modiolus is faintly visible (3L: ⇩). Normally, this area is hypointense due to both the bony structure of the modiolus and the cochlear nerve and spiral ganglion cells inside. However, here we have already determined from the CT images that there is no bony modiolus, so the hypointense signal in the central part of the cochlea that can be observed on the MRI is probably the cochlear nerve and spiral ganglion cells.

Patient 3-Dimensional Reconstructed MRI Findings

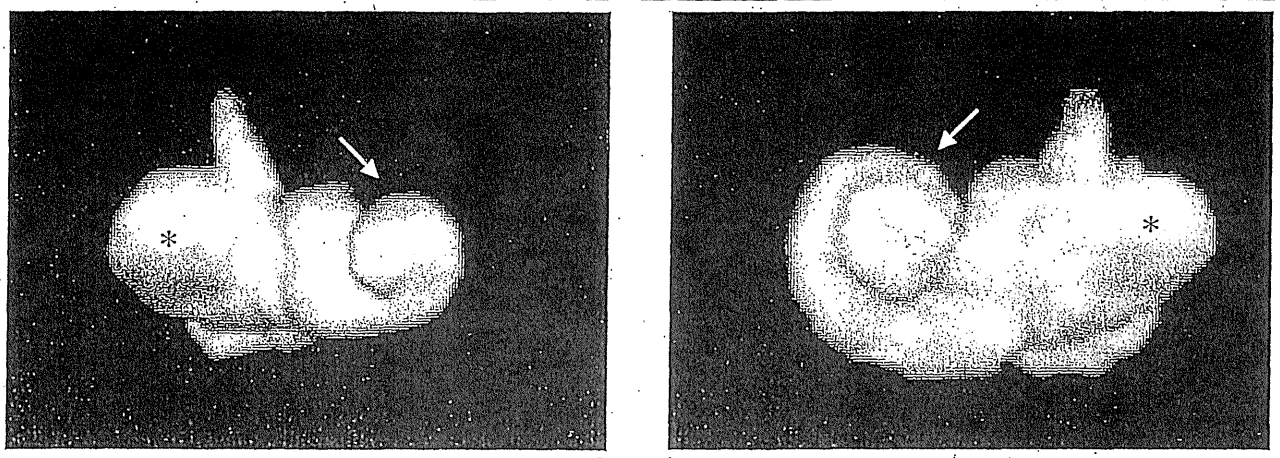

Fig. 37. (Case 6) 3-dimensional reconstructed MRI

[Patient 3-Dimensional Reconstructed MRI Findings]

Observing the 3-dimensional reconstructed MR images (R, L), the vestibular part (✻) is formed nearly the same on both sides. For the cochlea, however, whereas on the right side (R: ↘) the cochlea has approx. 1.5 turns overall and is cystic in the upper part, on the left side (L: ↙) the basal turn is almost completely formed and the second turn and beyond is cystic, leading us to believe that the left side is slightly more differentiated than the right.

Patient X-Ray Image Findings

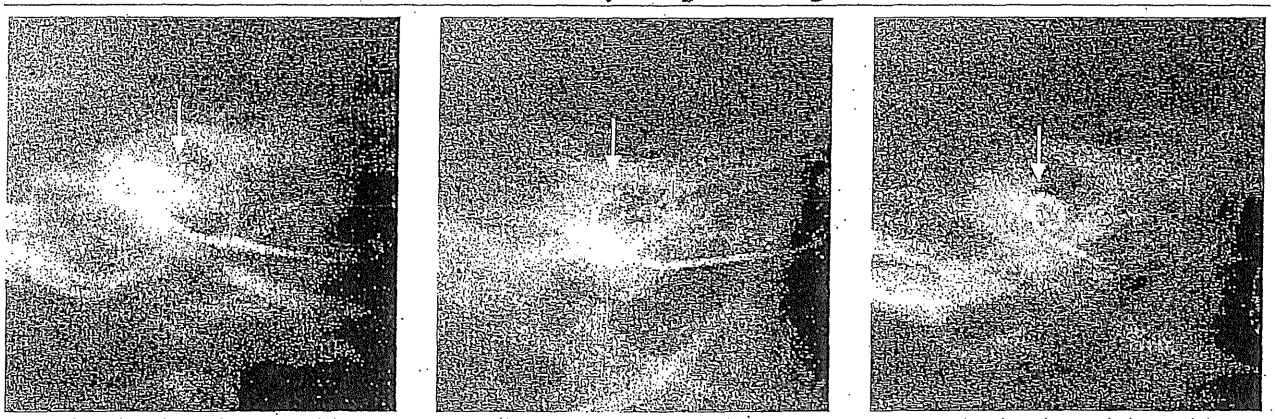

a. Initial implant (straight electrode)

b. Initial implant (same electrode as image left): facial spasms occurring

c. current implant (curved electrode)

Fig. 38. (Case 6) Postoperative X-ray images

[Patient X-Ray Image Findings]

In the intraoperative image taken during the initial surgery, full insertion could be confirmed (a: ↓), but in the image taken after the occurrence of facial spasms it was apparent that the electrode had slipped out slightly (b: ↓). The cochlear implant installed in the initial surgery was extracted, and this time a cochlear implant with a curved electrode was implanted (c: ↓).

Case 7 Incomplete Partition Type II (IP-II): Mondini Dysplasia (Enlarged Vestibular Aqueduct)

Subject: female, 7 years old

History and Clinical Findings

Newborn hearing screening revealed the need for further testing in both ears. The subject underwent hearing test and imaging and was diagnosed with moderate hearing loss accompanied by bilateral inner ear malformation. She was first examined by our department at three years ten months for detailed testing and evaluation of indication for a cochlear implant in the future. There were no findings of abnormality in the tympanic membranes in either ear, pure tone averages were 78.3 dB right and 93.3 dB left (fig. 39a), and spoken language had been favorably acquired through use of hearing aids in both ears, with no speech distortion. However, the subject's hearing level in both ears later showed a gradual decline, with repeated cycles of deterioration and improvement (fig. 39b), until at seven years for no particular reason hearing in both ears deteriorated, making it impossible for the subject to hear lessons at school or communicate with her peers, so she once again came to our department with her parents for consultation. At this time she exhibited bilateral deafness and completely lacked speech perception. After steroid therapy and follow-up study, cochlear implant surgery was performed on the left ear.

Patient CT Findings

There were no abnormalities of the external ear, middle ear, or ossicles in either ear. The findings presented are for the left ear, as findings for both ears were essentially the same. In the inner ear, whereas normally in the cochlea the structure of one or more turns can be identified after the second turn over the basal turn (fig. 40:n1, n2), in this case the basal turn is slightly thicker than normal and the upper turns form a single cavity with no partition visible between them and the modiolus (fig. 40:1). Examining the coronal image, it is readily apparent that the upper turns of the cochlea in this case are a single cystic mass (fig. 41:1). In the normal control image, observe that the structure is further divided in the second turn and beyond (fig. 41:n1). Overall 3-dimensional morphology of the inner ear will be covered in the MRI section.

The horizontal semicircular canal is slightly hypoplastic and the vestibule (fig. 40:2) is larger than normal (fig. 40:n2), but the most remarkable finding is the abnormally enlarged vestibular aqueduct. Normally the vestibular aqueduct is depicted as a line posterior to the posterior semicircular canal (fig. 40:n1, n2) and the endolymphatic sac cannot be directly observed, though it is positioned in a depression on the surface of the petrous bone (fig. 40:1). On the other hand, in this case the structure corresponding to the endolymphatic sac is clearly observable as a crevice on the posterior surface of the petrous part (fig. 40:1–3), and both the vestibular aqueduct itself and the opening to the posterior cranial fossa are extremely wide. Also, normally the origin of the vestibular aqueduct is exceedingly thin in the vestibule and invariably only partially depicted on a CT image, not becoming clearly visible until it has travelled several millimeters posteriorly (fig. 40:n3). In this case, though, one can plainly see the aqueduct leading directly mediposteriorly from the base of the common crus (fig. 40:3). However, the endolymphatic sac itself and its contents cannot be observed in the CT images because there is not enough density difference between them and the dura or the cerebrospinal fluid of the posterior cranial fossa posterior to them. The axial section diameter of the vestibular aqueduct in this case is 2.3 mm (fig. 40:4).

Patient MRI and 3-Dimensional Reconstructed MRI Findings

The clinically relevant points to focus attention on in the MR images for this case are the 3-dimensional morphology of the inner ear, the cochlear nerve, the vestibular aqueduct, and the endolymphatic sac.

First, examining the overall morphology of the inner ear, the insufficient turns of the cochlea could be diagnosed in the CT images, but can be more directly evaluated in the 3-dimensional reconstructed MRI. The basal turn of the cochlea in this case (fig. 41:2 ①) is little different from the normal control (fig. 41:n2 ①), but although in the normal control there is further structure (fig. 41:n2 *) superior to the second turn (fig. 41:n2 ②), in this case the area superior to the second turn is a single, cystic mass (fig. 41:2 ②).

The cochlear nerve is of normal thickness and clearly

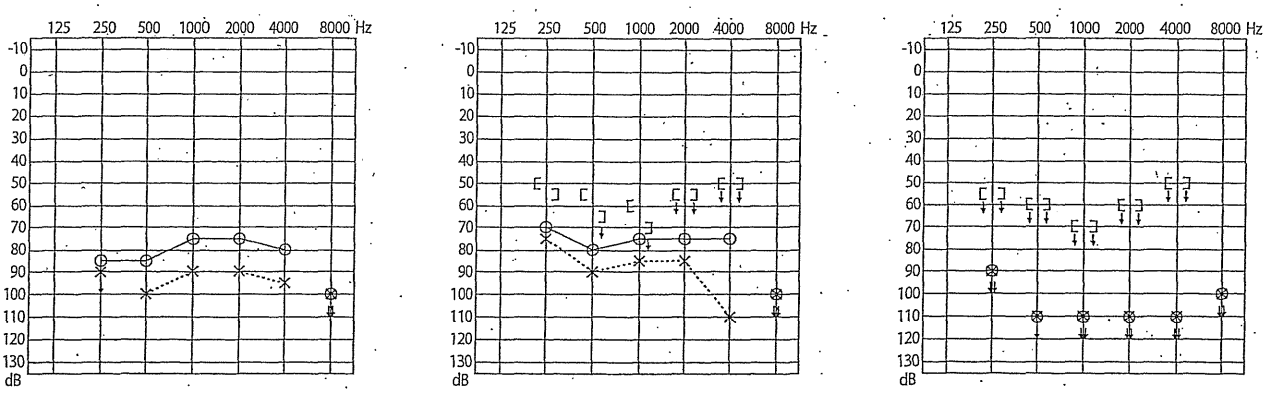

a. 3 years, 10 months b. 5 years, 10 months c. 7 years, 4 months

Fig. 39. (Case 7) Audiogram

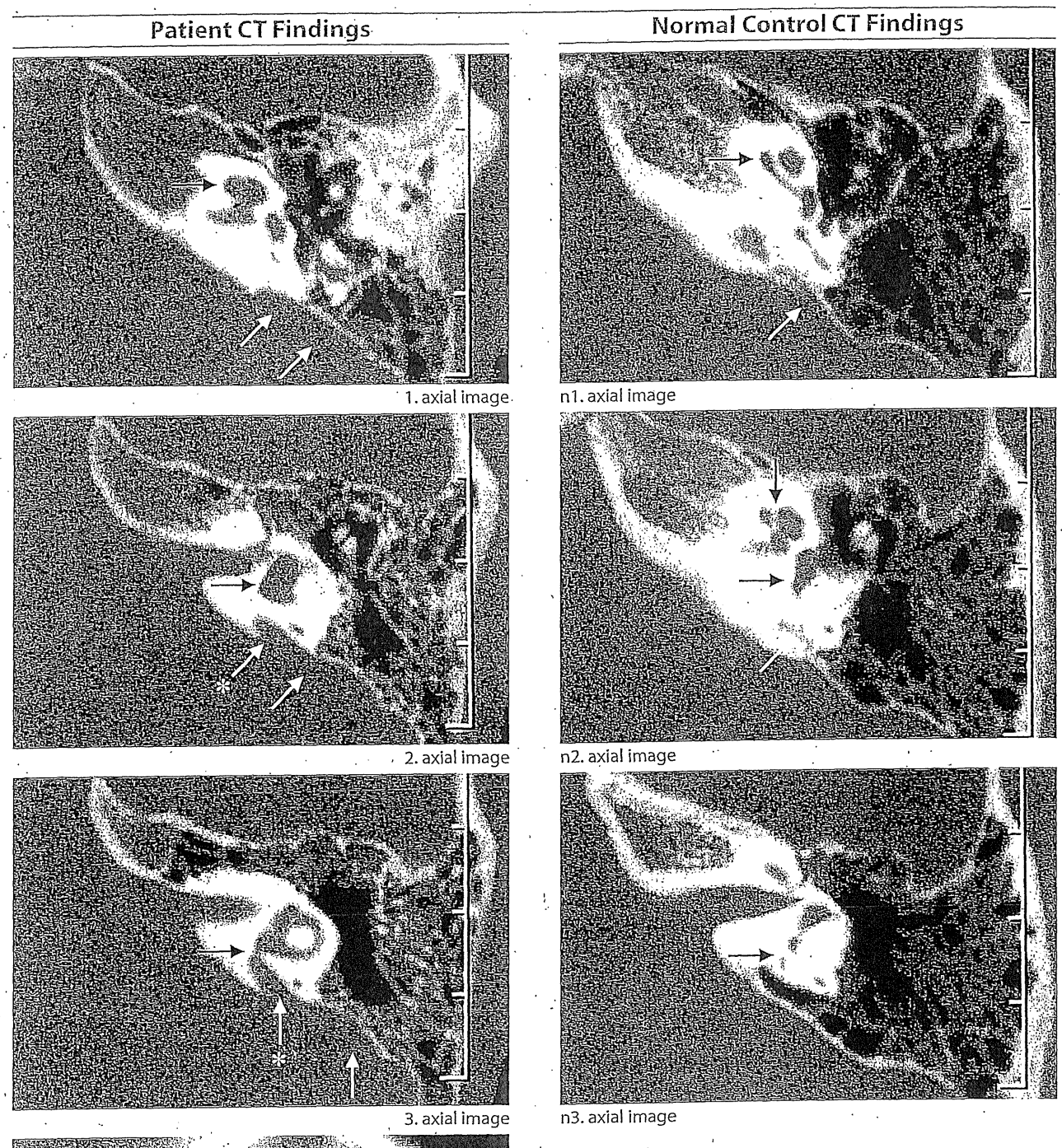

Fig. 40. (Case 7) CT

[Patient CT Findings]

In this case the basal turn of the cochlea is slightly thicker than normal and the upper turns form a single cavity with no partition visible between them and the modiolus (1: →). The horizontal semicircular canal is slightly hypoplastic and the vestibule (2: →) is larger than normal (n2: →), but the most remarkable finding is the abnormally enlarged vestibular aqueduct. In this case the structure corresponding to the endolymphatic sac is clearly visible as a crevice on the posterior surface of the petrous part (1–3: ↗), and both the vestibular aqueduct itself and the opening to the posterior cranial fossa are extremely wide (2, 3: ↗ with ❄). Also, one can plainly see the aqueduct leading directly mediposteriorly from the base of the common crus (3: →). The axial section diameter of the vestibular aqueduct in this case is 2.3 mm (4: ↙).

《Normal Control CT Findings》

The structure of one or more turns can be identified over the basal turn (n1: →, n2: ↓). n2: → vestibule; ↗ vestibular aqueduct. Normally the origin of the vestibular aqueduct is exceedingly thin in the vestibule and invariably only partially depicted on a CT image, not becoming clearly visible until it has travelled several millimeters posteriorly (n3: →).

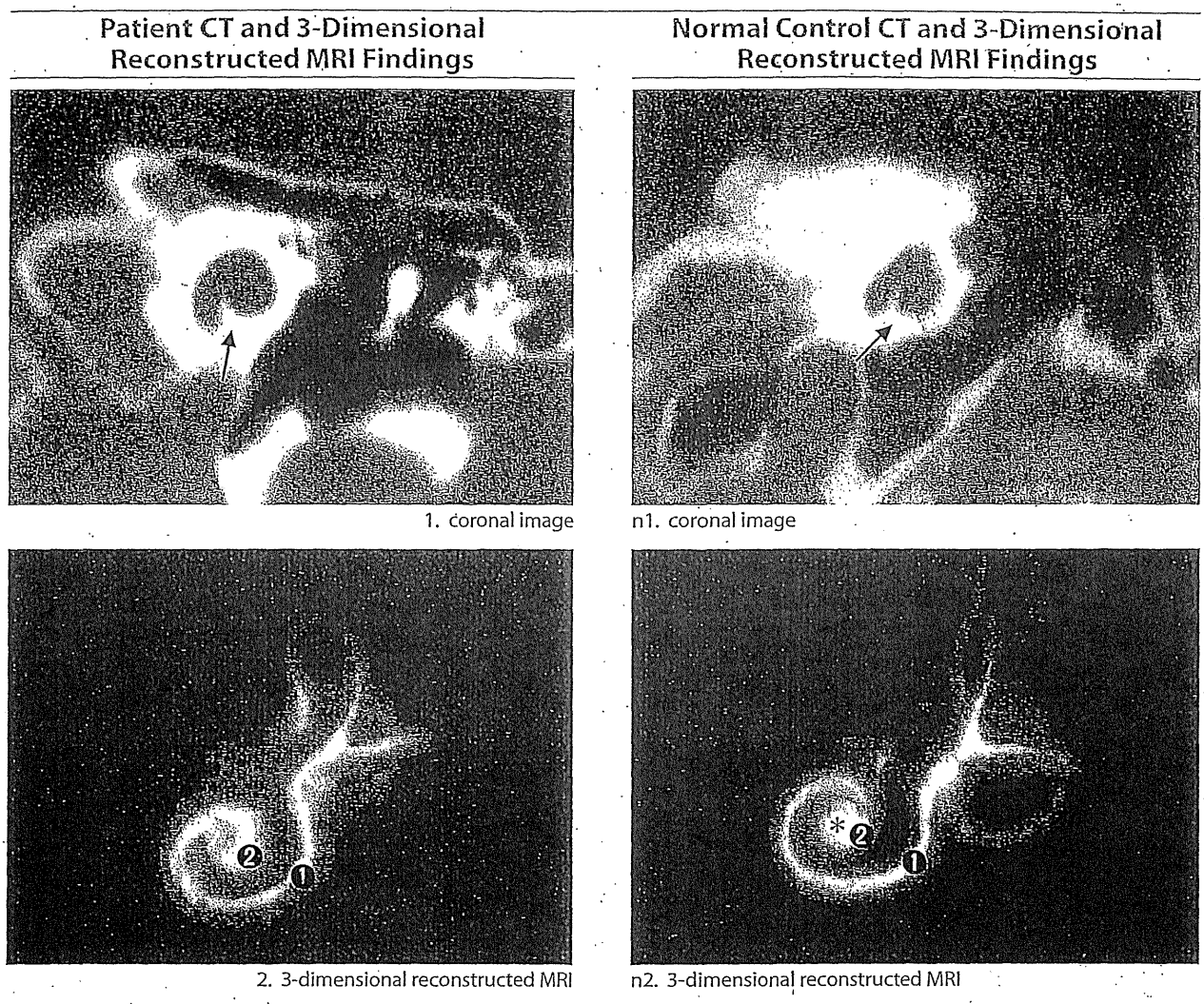

Fig. 41. (Case 7) CT and 3-dimensional reconstructed MRI

[Patient CT and 3-Dimensional Reconstructed MRI Findings]
It is clear that the upper turns of the cochlea form a single cavity (1:↑).The basal turn of the cochlea in this case (2 ①) is little different from the normal control (n2 ①), but although in the normal control there is further structure superior to the second turn (n2 ②), in this case the area superior to the second turn is a single, cystic mass (2 ②).

《Normal Control CT and 3-Dimensional Reconstructed MRI Findings》
In the normal cochlea, observe that the structure is further divided in the second turn and beyond (n1: ↗). n2: ① origin of basal turn; ② origin of second turn; * apical turn.

depicted (fig. 42:1). No atrophy or other abnormality can be ascertained, at least in the images, and the modiolus is also clearly visible (fig. 42:1). The fact that cochlear nerve morphology is normal suggests that we can expect electrical stimulation via a cochlear implant to be fully effective.

Furthermore, because the soft tissue contrast is much higher in the MRI than the CT images, it is possible to observe not only the vestibular aqueduct, but the endolymphatic sac itself. The endolymphatic sac in this case is T2 hyperintense and T1 hypointense in the proximal part, with similar intensity to cerebrospinal fluid, but in the distal part it is T1 isointense and T2 iso- to hypointense (fig. 42:1–3), indicating a possible accumulation of viscous fluid rich in protein, etc. In other words, we find that the characteristics of the fluid content vary depending on the part within the abnormally enlarged endolymphatic sac. Reports of this sort of accumulation of T1 hyperintense fluid in the endolymphatic sac in a case of enlarged vestibular aqueduct have already been seen elsewhere [1].

Surgical Findings

Cochlear implant surgery was performed on the left ear. There were no findings out of the ordinary during the mastoidectomy and posterior tympanotomy. Upon fenestration of the basal turn of the cochlea there was a pulsating discharge of lymph fluid, but the discharge ceased soon afterward. The cochlear implant, which employed a curved electrode that curls around the modiolus, was inserted as usual with no complications. Response of the cochlear nerve to cochlear implant stimulation during surgery was favorable.

The postoperative course was favorable, a broad dynamic range was obtained in cochlear implant mapping, and a final maximum discrimination score of 100% (monosyllabic speech perception test) was achieved.

Patient MRI Findings

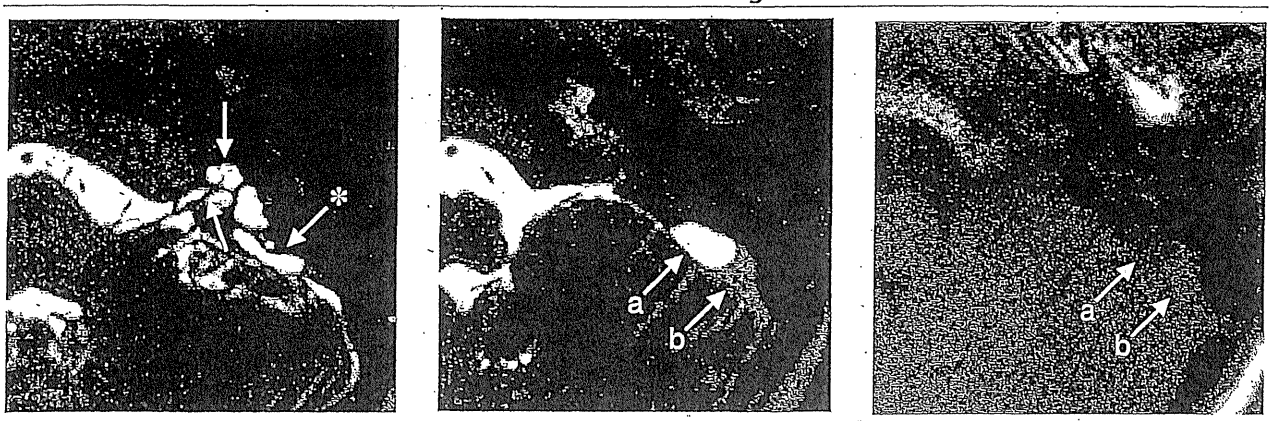

1 2 3

Fig. 42. (Case 7) MRI

[Patient MRI Findings]

The cochlear nerve is of normal thickness and clearly depicted (1: ↖). No atrophy or other abnormality can be ascertained, at least in the images, and the modiolus is also clearly visible (1: ↓). The endolymphatic sac is T2 hyperintense and T1 hypointense in the proximal part, with similar characteristics to cerebrospinal fluid (1: ❄↙; 2&3: a ↗), but in the distal part it is T1 isointense and T2 iso- to hypointense (2&3: b ↗), indicating a possible accumulation of viscous fluid rich in protein, etc.

Enlarged Vestibular Aqueduct Syndrome and the Anatomy of the Vestibular Aqueduct and Endolymphatic Sac

The vestibular aqueduct branches from the utricular and saccular ducts and exits from the medioposterior part of the vestibule, diverting medially around the common crus then running posterior to the posterior semicircular canal from medial to posterior before transitioning into the endolymphatic sac. The part of the vestibular aqueduct immediately after its origin in the medioposterior part of the vestibule is called the isthmus, or narrowest part. Ogura et al have reported [2] the measurement values for the vestibular aqueduct as follows: average overall length: 8.7 mm; average width at opening to posterior cranial fossa: 6.2 mm; average diameter at isthmus: 0.3 mm. The average spatial resolution for temporal bone CT images currently in general clinical use is around 0.3 mm on the XY plane and 0.6 mm in the Z direction, which are the settings of nearly all the CT images appearing in this book. Under these imaging conditions, it is difficult to clearly depict the isthmus of the vestibular aqueduct in the normal control sample due to the partial volume effect of the surrounding bony tissue. However, pathological enlargement of the vestibular aqueduct and endolymphatic sac can be clearly observed in CT images. The problem here is determining what degree of enlargement is abnormal. Valvassori and Clemis were the first to propose the disease concept of "large vestibular aqueduct syndrome" after examining the vestibular aqueduct in temporal bone tomograms and showing that, when the point midway between the common crus and the opening to the posterior surface of the petrous part had a diameter of 1.5 mm or greater, this constituted abnormal enlargement and such cases were almost always accompanied by hearing loss [3]. On the other hand, in a recent report by Madden et al, the condition of the vestibular aqueduct was measured in temporal bone CT axial images of cases with no sensorineural hearing loss due to injury, chronic otitis media, or other factors, viewing these vestibular aqueducts as 'normal samples.' The results indicated that 95th percentile values for diameters of the vestibular aqueduct at its midpoint and at the opercular part where it opens into the posterior cranial fossa were 0.8 mm and 1.7 mm, respectively, with diameters of 0.9 mm or greater at the midpoint of the vestibular aqueduct and 1.8 mm or greater at the opercular part considered abnormal enlargement [4]. Other standards used, for example those in the paper by Colvin et al, define abnormal vestibular aqueduct enlargement as a diameter of 2.0 mm or greater at the midpoint of the vestibular aqueduct alone with enlargement of the ipsilateral endolymphatic sac, or a midpoint diameter of 1.4 mm or greater if the midpoint diameter on the contralateral side is 2.0 mm or more [5]. In actual clinical practice there is almost never a doubt as to whether or not enlarged vestibular aqueduct syndrome is present, but, as discussed below, since there is no single cause for this syndrome one would expect to find cases approaching the borderline between normal and abnormal. In such cases, it is necessary to take measurements using CT or MR images, compare them to standards such as those presented here, and make a quantitative decision.

Also, on a minor note concerning nomenclature used in this case, what was initially referred to here as "large vestibular aqueduct" or LVA, is recently more commonly referred to as "enlarged vestibular aqueduct" or EVA. Naturally, they refer to the same pathological condition and the terms can be used interchangeably.

Enlarged vestibular aqueduct is the most common inner ear malformation, and in addition to congenital hearing loss there are many cases of progressive hearing loss after birth. Gradual loss of hearing is more common, but in approx. ⅓ of cases the hearing loss is sudden. Of these, there are reports that nearly 80% are triggered by events such as a blow to the head, exercise, or common colds [5]. Some affected children, particularly those whose hearing is near the borderline for hearing aid

effectiveness, are discouraged from participating in activities that involve strong head movements. As for vestibular symptoms, worsening hearing loss is frequently accompanied by vertigo, indicating that the condition is one that extends to the entire inner ear. In serious cases, simply inclining the head can sometimes give rise to rotary vertigo. Particularly in young children, care should be taken not to be distracted by attendant symptoms of nausea and vomiting, while overlooking the vertigo and nystagmus. From personal experience, I had a case which for many years was diagnosed as autointoxication. Hearing loss was essentially sensorineural, but on examination of the details one found mixed hearing loss with an air-bone gap of 20–30 dB in the low frequency range. One cause of this may have been that excessive endolymph volume increased inertial mass, limiting the mobility of the footplate of the stapes [6].

Based on MRI findings and the surgical findings described below, the content of the enlarged portion of the vestibular aqueduct and endolymphatic sac can be regarded as composed mainly of lymph from the endolymphatic space. When I have performed closure surgery on the vestibular aqueduct and endolymphatic sac in order to control vertigo in cases of enlarged vestibular aqueduct syndrome, fluid extracted from the endolymphatic sac was pale yellow and transparent. The electrolyte composition, which in endolymph would normally be high in potassium, had Na, K, and Cl densities of 140, 5.1, and 109 (mEq/l) respectively—the same low-potassium composition as normal perilymphatic fluid. On the other hand, when conducting a scala tympani fenestration of the basal turn of the cochlea during cochlear implantation in cases of enlarged vestibular aqueduct syndrome, the initial strong, pulsating discharge of labyrinthine fluid stops naturally after a while. In cases not involving enlarged vestibular aqueduct the volume of inner ear fluid (perilymph) discharged is minimal, with little or no pulsation. This finding indicates that in enlarged vestibular aqueduct syndrome intracranial pressure exerted on the endolymphatic sac from the posterior cranial fossa is directly transmitted to the cochlea, and the volume of discharge implies that the large quantity of endolymph in the endolymphatic sac and vestibular aqueduct is diverted from perilymphatic space in the cochlea and discharged from the scala tympani. However, as seen in Case 7, the fluid in the endolymphatic sac can sometimes be viscous fluid that is T2 hypointense or T1 isointense, and it is possible that this could work to impair the inner ear. On the other hand, there are reports that there is no relationship between the width (midpoint diameter) of the enlarged vestibular aqueduct and long-range deterioration of hearing—that is, it does not follow that the thicker the vestibular aqueduct the easier it is for hearing loss to worsen [5] —which suggests that the progression of hearing loss cannot be explained through the physical causes of pressure transmission from the vestibular aqueduct to the inner ear or reflux of high-density fluid alone.

Concerning the etiology of the case shown here, based on linkage analysis and genetic mutation screening, it is clear that a mutation of the responsible gene (SLC26A4/PDS) for Pendred syndrome (a syndrome accompanied by hearing loss and goiter) can give rise to non-syndromic hearing loss different from the phenotype [3, 7], but reports vary widely on the frequency of enlarged vestibular aqueduct syndrome with recognized SLC26A4 genetic mutation, from around 30–90% [4, 8]. With SLC26A4 genetic mutation, it has been reported that enlargement of the vestibular aqueduct is greater when two alleles are affected than just one allele and that the hearing loss is more severe [4, 8]. Considering both that the SLC26A4 gene is expressed in the stria vascularis of the inner ear, the endolymphatic sac and endolymphatic duct, the vicinity of the vestibular macula and lateral scala media of the cochlea and that there is no correlation between the degree of hearing loss and the anatomical enlargement of the vestibular aqueduct alone, it can be surmised that the mechanism through which the SLC26A4 gene directly influences inner ear function by maintaining endolymph homeostasis and endocochlear potential [9] also plays an important role in the onset of hearing loss. On the other hand, even in clear cases of enlarged vestibular aqueduct syndrome, in many cases the SLC26A4 mutation is negative, and there are also reports of enlarged vestibular aqueduct syndrome with combined mutations in SLC26A4 and GJB2 [4]. These observations indicate that not one, but several factors bring about the common morphological abnormality of vestibular aqueduct enlargement, and this can be assumed to be one of the reasons for the variety of clinical manifestations.

Cochlear Implant Surgical Indication in Cases of Enlarged Vestibular Aqueduct Syndrome

When conducting cochlear implantation for conditions such as in Case 7, there are two approaches in determining on which side to perform the surgery. With the first approach, considering the fact that during the course of treatment to date hearing has been quite consistently favorable in the right ear, there is a possibility that if hearing improves a hearing aid can be used effectively on this side, so cochlear implant surgery should be performed on the opposite, left ear. With the other approach, on the assumption that since hearing is relatively better in the right ear the condition of the auditory nerve must also be favorable, cochlear implant surgery should be performed on the right ear where conditions are slightly better. Taking into consideration that, in the long term, hearing in the right ear may be lost completely with no chance of improvement, the second option may seem more rational, but if right ear hearing does improve and a hearing aid can be effectively used, there is a possibility of attaining binaural hearing even if only for a limited time. Also, given that on average the effectiveness of cochlear implants in cases of enlarged vestibular aqueduct syndrome is favorable [10], it is possible that there will be no significant difference in the postoperative effectiveness of the cochlear implant. It is up to the patient and parents to determine the timing and side of the surgery among themselves after receiving a complete explanation from the attending physician concerning the factors described above. With this disease, cochlear implantation often becomes necessary at school age, and considering the isolation and effect on studies experienced by a child with severe hearing loss, a more positive principle on the surgical indication may be appropriate.

References

1 Sugiura M, Naganawa S, Sato E, Nakashima T: Visualization of a high protein concentration in the cochlea of a patient with a large endolymphatic duct and sac, using three-dimensional fluid-attenuated inversion recovery magnetic resonance imaging. J Laryngol Otol 2006; 120:1084–1086.
2 Ogura Y, Clemis JD: A study of the gross anatomy of the human vestibular aqueduct. Ann Otol Rhinol Laryngol 1971;80:813–825.
3 Valvassori GE, Clemis JD: The large vestibular aqueduct syndrome. Laryngoscope 1978;88:723–728.
4 Madden C, Halsted M, Meinzen-Derr J, et al: The influence of mutation in the SLC26A4 gene on the temporal bone in a population with enlarged vestibular aqueduct. Arch Otolaryngol Head Neck Surg 2007;133:162–168.
5 Colvin IB, Beale T, Harrop-Griffiths K: Long-term follow-up of hearing loss in children and young adults with enlarged vestibular aqueducts: Relationship to radiologic findings and Pendred syndrome diagnosis. Laryngoscope 2006;116:2027–2036.
6 Sato E, Nakashima T, Lilly DJ, et al: Tympanometric findings in patients with enlarged vestibular aqueducts. Laryngoscope 2002; 112:1642–1646.
7 Usami S, Abe S, Weston MD, et al: Non-syndromic hearing loss associated with enlarged vestibular aqueduct is caused by PDS mutations. Hum Genet 1999;104:188–192.
8 Okamoto Y, Matsunaga T, Taiji H, et al: Mutation of SLC26A4 are associated with the clinical features in patients with bilateral enlargement of the vestibular aqueduct. Audiology Japan 2010;53:164–170.
9 Royaux IE, Belyantseva IA, Wu T, et al: Localization and functional studies of pendrin in the mouse inner ear provide insight about the etiology of deafness in pendred syndrome. J Assoc Res Otolaryngol 2003;4:394–404.
10 Buchman CA, Copeland BJ, Yu KK, et al: Cochlear implantation in children with congenital inner ear malformations. Laryngoscope 2004;114:309–316.

Points

1. In cases of sensorineural hearing loss that progresses in childhood, suspect enlarged vestibular aqueduct syndrome.
2. Enlarged vestibular aqueduct syndrome is sometimes accompanied by other inner ear malformations and sometimes arises independently.
3. With this condition the vestibular aqueduct can be observed leading directly from the vestibule, which is not possible in normal images.
4. SLC26A4 genetic mutation is an important causative factor.

Case 8

Incomplete Partition Type III (IP-III)

Subject: male, 2 years, 11 months

History and Clinical Findings

The parents first took the subject to the ENT department of a local hospital after noticing that he did not respond clearly to sound. The child exhibited speech retardation and the ABR thresholds were 60 to 70 dB SPL in both ears. He had been using hearing aids bilaterally since confirmation of severe hearing loss, but speech development was unsatisfactory and he was referred to our department for further examination and possible surgical treatment.

The ASSR thresholds as examined in our department were approx. 90 dB in both ears, which were approx. 20 dB higher than previous ABR thresholds, suggesting progressive hearing deterioration. Hearing thresholds examined with conditioned orientation reflex audiometry were approx. 85 dB, and aided thresholds were between 45 and 65 dB. Developmental testing showed normal Cognitive-Adaptive development (developmental quotient: DQ 100), while Language-Social development was apparently delayed (DQ 50). The subject understood around 50 spoken words and could speak several meaningful words, but the phonation was excessively nasalized. Genetic testing for hearing loss has not yet been performed. There is no history of hearing loss among the subject's parents or relatives, and he is an only child. Temporal bone CT and MRI examinations were performed to search for the etiology of the patient's hearing loss.

Patient CT Findings

CT and MRI findings are the same in both ears. The images for the left ear are shown. The mastoid air cells are well developed and no abnormal soft tissue density is observed in the middle ear in the temporal bone CT. No anomalies can be identified in the middle ear, including the ossicular chains. In the inner ear, the interscalar septa of the cochlea are partially present, but the bony modiolus is completely absent, along with the septum between the cochlea and the internal auditory canal (fig. 43:1). The internal auditory canal directly communicates with the cochlea at its lateral end (fig. 43:1). The vestibule and semicircular canals appear normal, but the bony canal for the superior vestibular nerve is larger than normal (fig. 43:2). In addition, the labyrinthine segment of the facial nerve is located superior to the cochlea (fig. 43:3), which may be due to the abnormally inferior and posterior location of the cochlea in this patient.

Patient MRI Findings

Three-dimensional reconstructed MRI of the inner ear shows a poorly separated cochlear duct (fig. 44:1) and enlarged internal auditory canal (fig. 44:1). T2 weighted high resolution MRI reveals the cochlea as a high intensity area, and the low intensity structure corresponding to the cochlear nerve in the modiolus can also be identified (fig. 45:1). The bifurcation between the cochlear nerve and the vestibular nerve can be identified in the internal auditory canal (fig. 45:2) in the same way as in the normal control (fig. 45:n2). The diameter of the superior

Patient CT Findings

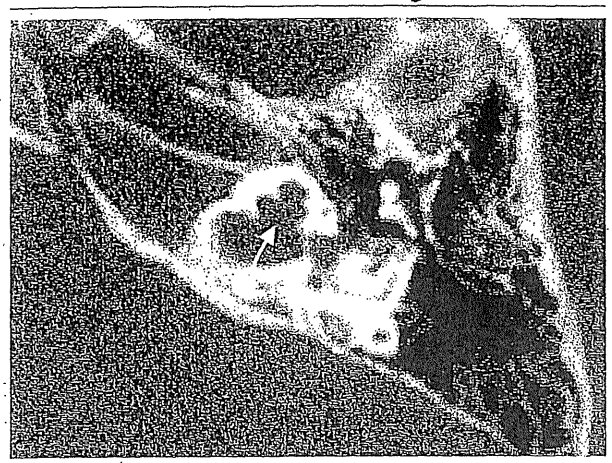

1. axial image

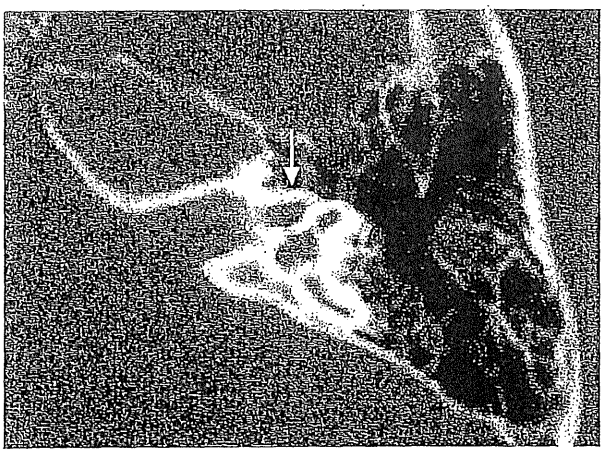

2. axial image

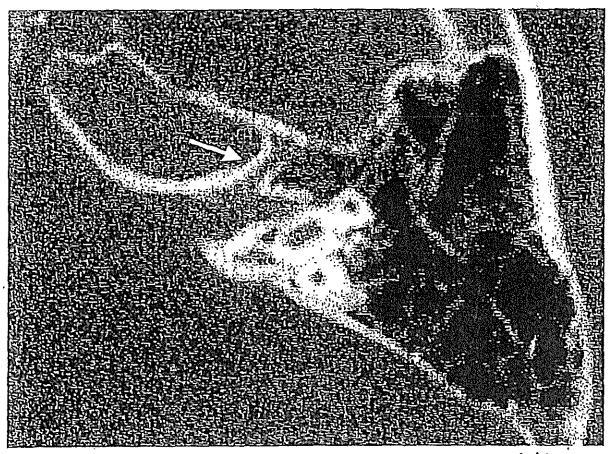

3. axial image

Normal Control CT Findings

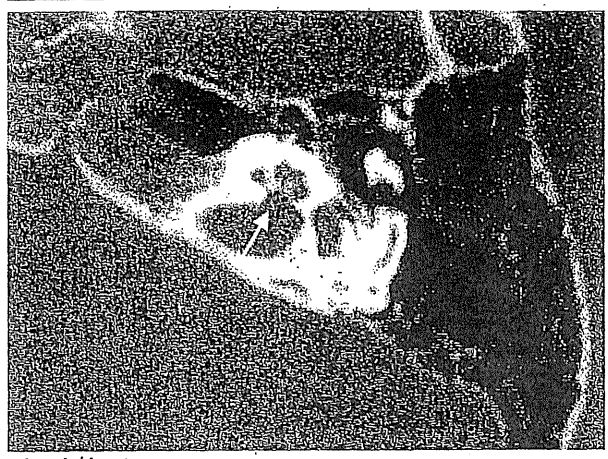

n1. axial image

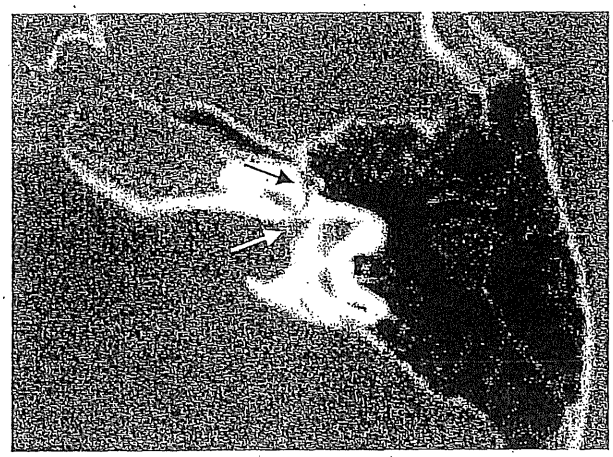

n2. axial image

Fig. 43. (Case 8) CT

[Patient CT Findings]

The mastoid air cells are well developed and no abnormal soft tissue density is observed in the middle ear in the temporal bone CT. No anomalies can be identified in the middle ear, including the ossicular chains. In the inner ear, the interscalar septa of the cochlea are partially present, but the bony modiolus is completely absent, along with the septum between the cochlea and the internal auditory canal (1:). In the normal control, the modiolus and the bony septum at the base of the modiolus are clearly depicted (n1:). The internal auditory canal directly communicates with the cochlea at its lateral end (1:). The vestibule and semicircular canals appear normal, but the bony canal for the superior vestibular nerve is larger than normal (2:). In addition, the labyrinthine segment of the facial nerve is located superior to the cochlea (3:), which may be due to the abnormally inferior and posterior location of the cochlea in this patient. In contrast, in the normal control image, the labyrinthine segment of the facial nerve is observed in the same section as the most superior part of the cochlear basal turn (n2:), and the bony canal for the superior vestibular nerve (n2:) is smaller than that of this patient.

vestibular nerve canal is large, inside of which the superior vestibular nerve can be observed as a low-intensity line (fig. 45:3). The hypointense septum between the cochlea and the internal auditory canal, however, is not visible.

Clinical Course

The patient is being followed up in our department, and his hearing, speech perception, and expression skills are being checked continuously to find out whether the hearing aids are effectively helping the child with his spoken language development. Cochlear implantation will be indicated if the progress of his speech development is too slow, or if pure tone hearing deteriorates further.

Incomplete Partition Type III (IP-III) Anomaly of the Inner Ear

IP-III is an X-linked inner ear anomaly that is marked by the absence of the bony modiolus and of the septum between the base of the cochlea and the internal auditory canal [1, 2]. The bony interscalar septa are partially present and the external dimensions of the cochlea do not differ from normal [1, 2]. In contrast, no anomalies are identified in the vestibular part of the inner ear. The soft tissue structures such as the cochlear nerve, vestibular nerve, and facial nerves appear normal in MR images. Cochlear implantation in a patient with this anomaly is possible and may show good postoperative performance, but requires utmost attention since a cerebrospinal fluid (CSF) gusher is inevitable [3] and there is a risk of aberrant electrode array insertion into the internal auditory canal. For details, see the following special article on IP-III by Professor Sennaroglu (Please see p.106).

References

1 Sennaroglu L, Sarac S, Ergin T: Surgical results of cochlear implantation in malformed cochlea. Otol Neurotol 2006;27:615–623.

2 Sennaroglu L: Cochlear implantation in inner ear malformations—a review article. Cochlear Implants Int 2010;11:4–41.

3 Incesulu A, Adapinar B, Kecik C: Cochlear implantation in cases with incomplete partition type III (X-linked anomaly). Eur Arch Otorhinolaryngol 2008;265:1425–1430.

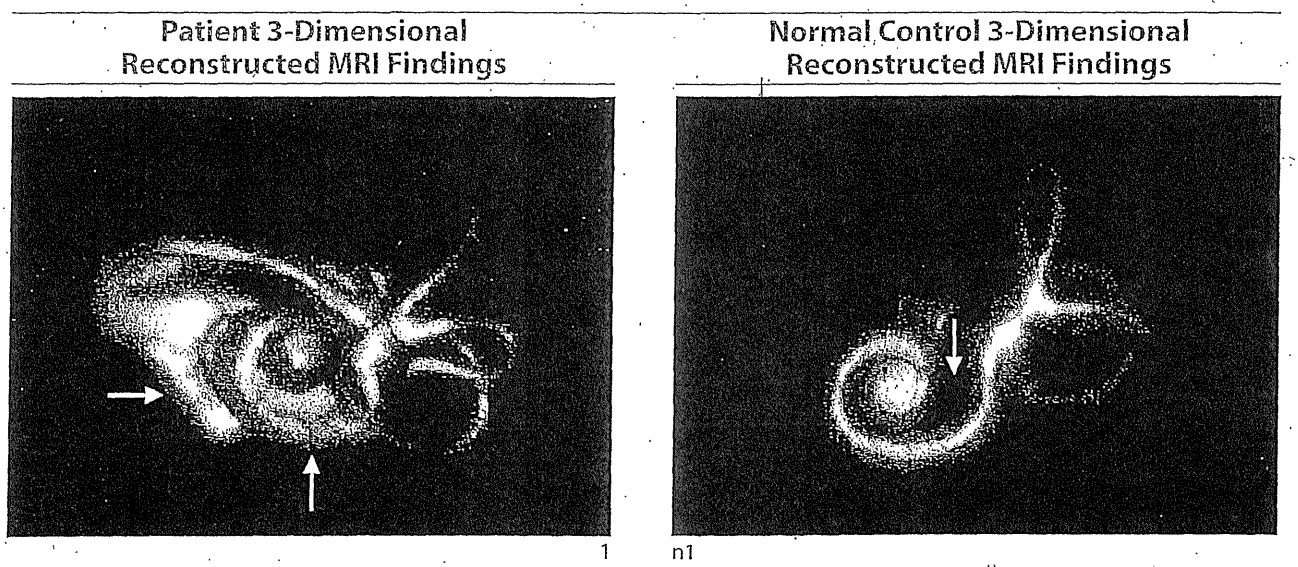

Fig. 44. (Case 8) 3-dimensional reconstructed MRI

[Patient 3-Dimensional Reconstructed MRI Findings]
Three-dimensional reconstructed MRI of the inner ear shows a poorly separated cochlear duct (1: ⇑) and enlarged internal auditory canal (1: ⇨). In a normal cochlea, the upper turn is clearly separated from the basal turn (n1: ⇓).

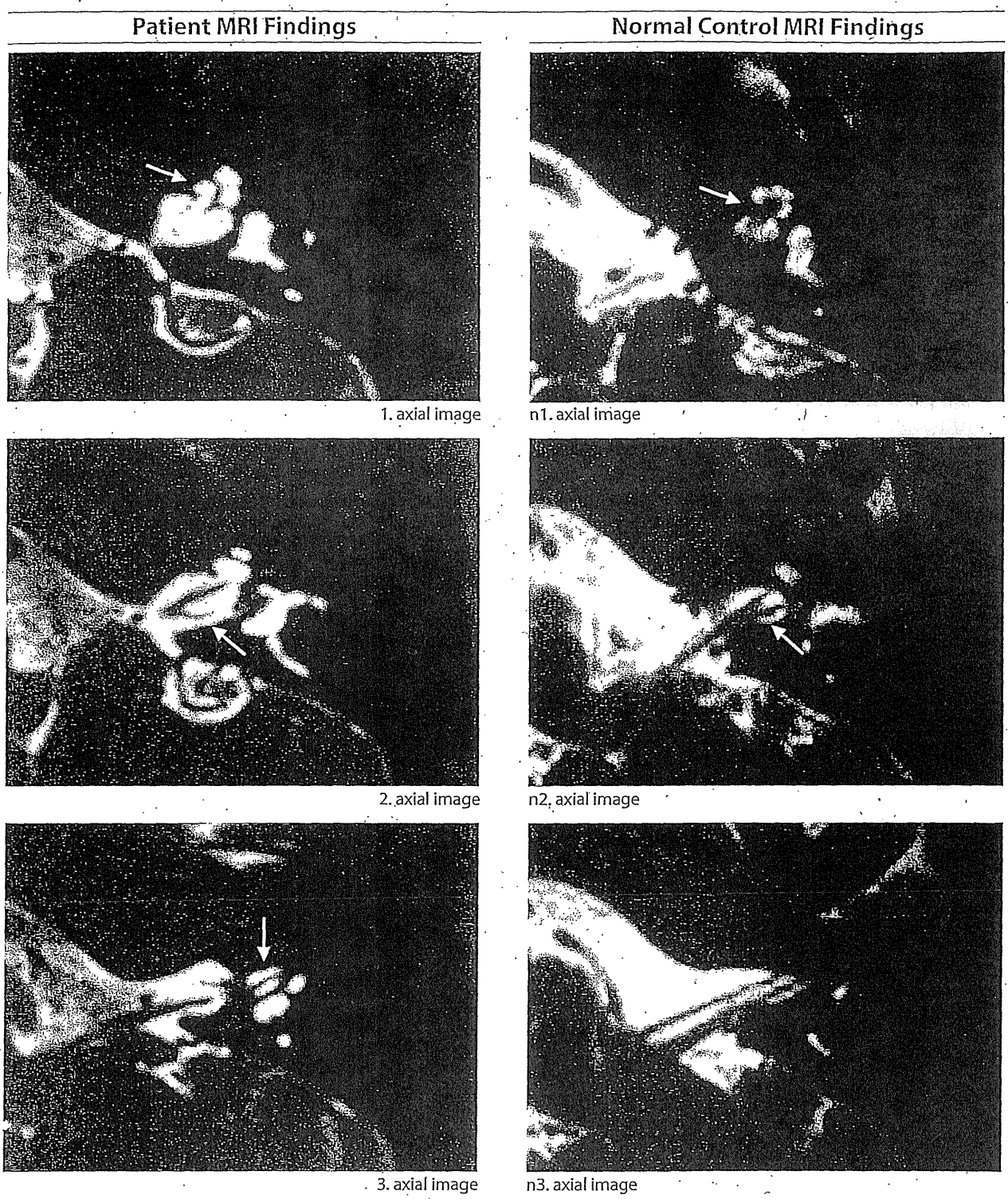

Fig. 45. (Case 8) MRI

[Patient MRI Findings]

T2 weighted high resolution MRI reveals the cochlea as a high intensity area, and the low intensity structure corresponding to the cochlear nerve in the modiolus can also be identified (1: ⇨). The bifurcation between the cochlear nerve and the vestibular nerve can be identified in the internal auditory canal (2: ⇖) in the same way as in the normal control (n2 ⇖). The diameter of the superior vestibular nerve canal is large, inside of which the superior vestibular nerve can be observed as a low-intensity line (3: ⇩). The hypointense septum between the cochlea and the internal auditory canal, which can be identified in normal control (n1: ⇨), however, is not visible (1).

Special Article

Incomplete Partition Type III

Levent Sennaroglu, M.D.

Professor of Otolaryngology, Department of Otolaryngology
Hacettepe University Medical Faculty
Ankara, Turkey

Incomplete partition type III cochlear malformation is the type of anomaly present in X-linked deafness which was described by Nance et al [1] for the first time in 1971. They reported that the X-linked transmission of congenital mixed hearing loss is associated with a fixed stapes footplate and perilymph gusher during attempted stapedectomy. Although mainly seen in males they indicated that female heterozygotes had similar but milder audiological abnormalities. Later Papadaki et al [2] reported two cases of X-linked deafness with stapes gusher in females with normal male relatives. Bulbous dilatation of the fundus of the internal auditory canals (IAC), incomplete separation of the IAC from the base of the cochlea, and widened facial nerve canals were seen in both female patients.

There may be different ways of clinical presentation: sensorineural hearing loss (SNHL) or mixed type hearing loss. It is not infrequent to see air-bone gap in these patients. Bento and Miniti [3] reported four cases where hearing aid use was impossible. One of them was explored for stapedectomy. During the removal of the footplate there was severe gusher where a piston placement was impossible. Similar cases who had severe gusher during stapedetomy were reported in the literature [4, 5]. In those cases either the piston could not be placed or there were further SNHL. It appears from the experience of these authors that stapedectomy is to be avoided in this group of patients.

Genetics

According to de Kok et al [6] the underlying DFN3 gene (deafness with congenital stapes footplate fixation) has been mapped to the Xq21 region, and is caused by mutations in or around the POU3F4 gene. Female obligate carriers may be normal, or have a milder form of the same anomaly associated with milder hearing loss [7].

Audiological Features

The patients usually apply with hearing loss. There may be two different forms of presentation:

1-Mixed Type Hearing Loss:

SNHL component is most probably due to the modiolar defect. The air-bone gap observed in our patients usually involves high frequencies as well as low frequencies. Conductive component is due to stapedial fixation. Snik et al. [8] reported that if the degree of hearing loss was not too much, stapedius reflex could be obtained in this group of patients.

Tang et al [9] have a different explanation for the conductive hearing loss. They are in the opinion that the intracranial pressure is transmitted into the perilymphatic space, and the raised perilymphatic pressure that is exerted on the cochlear duct and the stapes footplate results in a mixed pattern of sensorineural and conductive hearing loss respectively.

Snik et al [8] explained the air-bone gap with the third window phenomenon. They reported that because of the congenital malformation audiovestibular system functioned more effective than normal system leading to better bone conduction levels. Their study revealed that audiological studies were in accordance with pure sensorineural hearing loss and air-bone gap in the audiogram did not have the significance of conductive hearing loss component.

2-The other common form of presentation is profound SNHL, where the severity may vary. This is most probably due to the absence of the modiolus and in this situation cochlear implant (CI) surgery is the option for restoring hearing. All three patients followed in our department had severe to profound SNHL and underwent CI surgery.

Radiology

The cochlea in incomplete partition type III has interscalar septa but the modiolus is completely absent (fig. 46:a, b).

This anomaly is the rarest form of incomplete partition cases. According to the radiological database in Hacettepe University Department of Otolaryngology incomplete partition cases are 41% of the whole inner ear malformations. IP-III constitutes 2% of the inner ear malformation group. So far only three patients received CI in Hacettepe University and one patient is being followed with hearing aid.

Radiological appearance of a cochlea with incomplete partition type III is very characteristic. HRCT findings were described elegantly by Phelps et al [7] for the first time, but this characteristic deformity was included under the category of incomplete partition deformities for the first time by Sennaroglu et al [10] in 2006.

Phelps et al [7] reported three main features of this rare disorder:

(1) bulbous internal auditory canal,
(2) incomplete separation of the coils of the cochlea from the internal auditory canal and
(3) wide first and second parts of the intratemporal facial nerve canal with a less acute angle between them.

Talbot and Wilson [5] later added that modiolus is absent in these patients. Later papers confirmed the existence of these deformities in other patient groups as well. Chee et al [11] mentioned bilateral and symmetric bulbous dilatation of the internal auditory canals. Kumar et al [4] reported that the labyrinthine segments of the facial nerve canals also appeared enlarged bilaterally.

Apart from these three features a more medial origin of the vestibular aqueduct with varying degree of dilatation was described by Talbot and Wilson [5]. Kumar et al [4] recently reported that this was not seen in their patient and has not been reported in any other patients. This feature is also seen bilaterally in one of our patients too.

In addition to these features the present author noticed

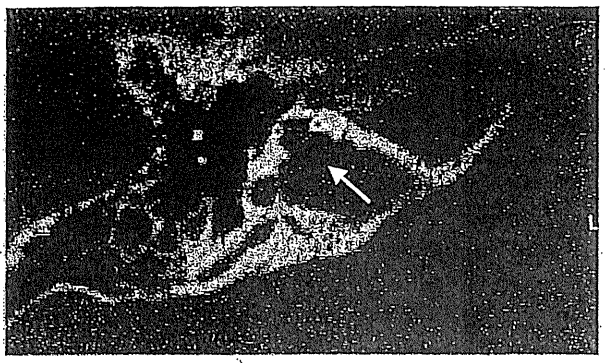

a. Axial section showing cochlea with incomplete partition type III deformity. It is possible to visualize interscalar septa (*), however there is a large defect at the base of the cochlea (↖).

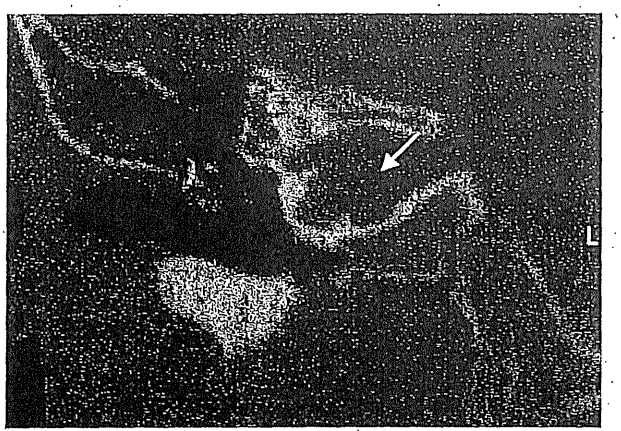

b. Coronal section with a defect at the base of the cochlea (↙).

Fig. 46

that in this deformity the interscalar septa are present but the modiolus is completely absent [12] (fig. 46:a, b). The cochlea was placed directly at the lateral end of the internal auditory canal instead of its usual anterolateral position. This gives the cochlea a characteristic appearance. From an earlier study the external dimensions of the cochlea (height and diameter) were found to be similar to normal cochlea [10]. Apart from these features the present author noticed that labyrinthine segment of the facial nerve has a more superior position in relation to cochlea; labyrinthine segment is located almost above the cochlea. If the axial sections are followed from top to bottom, the first structure is the labyrinthine segment of the facial nerve. In addition there is a very thin otic capsule around the cochlea and vestibule.

Talbot and Wilson [5] suggested that young males with congenital mixed type hearing loss should be studied with high resolution CT of the temporal bone. This is a very important suggestion that should be done.

Surgical Treatment

Incomplete Partition (IP) malformations have normal external dimensions but internal architecture is defective with variable degrees. The external dimensions of the cochlea (height and diameter) are not different from a normal cochlea. IP-I and IP-III have a defect at the base and this creates a route for cerebrospinal fluid (CSF) to fill the cochlea. Modiolus is partially present in IP-II and here the defect is less compared to IP-I and IP-III. Therefore, during surgery of IP-I and IP-III there is a high likelihood of severe CSF gusher. In IP-II gusher is rare but oozing is more common. Therefore, during the surgery of IP-III two serious problems may occur:

1-gusher during cochleostomy
2-electrode misplacement into the IAC

The surgeon must be ready to cope with these problems. During electrode choice these factors should be kept in mind. Because of the defective modiolus electrodes with complete rings or contact surface on both sides may provide better stimulation. The probability of the longer electrodes entering the IAC is more than the shorter electrodes. Therefore, an electrode with full rings or contact surfaces on both sides that will make only one turn around the cochlea appears to be sufficient.

Modiolar hugging electrodes may have a tendency going towards the center of the cochlea. In IP-III this may result in misplacement into the IAC. Because of its length, Med El standard electrode may also go into the IAC. Therefore, Med El compressed array, and Nucleus 24 K appear to be options. The author developed an electrode with a "cork" type stopper (standard electrode 25 mm) appears to be ideal for these cases by properly sealing the cochleostomy (to prevent CSF fistula postoperatively) and also making one full turn around the cochlea,

A-Gusher:

These patients have severe gusher during surgery. If it is not properly sealed the postoperative CSF leakage may lead to recurrent meningitis. Ideally the size of the cochleostomy should be slightly larger than the electrode allowing a soft tissue to be placed around the electrode. Passing the electrode through a tiny piece of fascia and inserting this together with the electrode may have even a better seal at the cochleostomy.

The electrode with "Cork" type stopper has the following features: It has a "cork" like stopper instead of the usual silicon ring at the end of the intracochlear electrode to prevent CSF fistula after CI insertion. This was designed to close the cochleostomy more efficiently to stop the escape of CSF around the electrode. The diameter of the "cork" stopper is 1.9 mm. The diameter of the active electrode is 1 mm. A cochleostomy should be created with a burr size of 1.2 mm. This allows the active electrode to pass through without resistance, without letting the stopper with a diameter of 1.9 mm to pass through; thereby effectively closing the cochleostomy. The length of the electrode is 25 mm, to make one full turn around the cochlea. This is the standard "cork". (fig. 47a) electrode where contact spacing between active electrodes is 1.7 mm. It also has contact surfaces on both sides of the electrode for more effective stimulation rather than electrodes with half banded contacts facing the modiolus. Intraoperative radiology should be obtained in order to check the position of the electrode which is expected to be round shape following the contour of the cochlea (fig. 47b).

It is important to use the tissue glue after each layer of soft tissue added. After the first layer of soft tissue is placed, a little amount of tissue glue is added to fix this

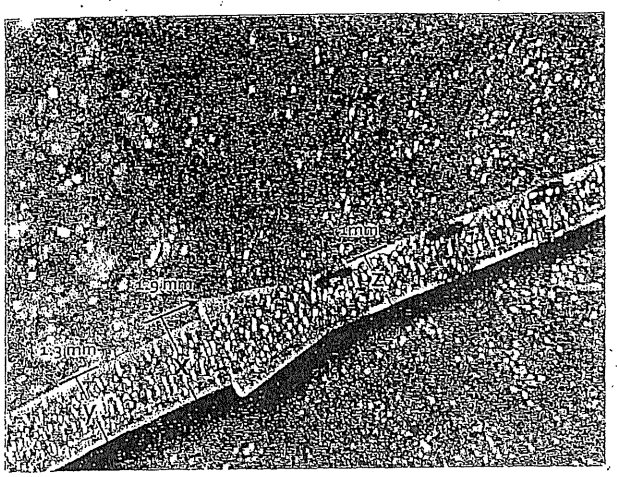

a. Electrode with cork stopper.

b. Transorbital view showing cork electrode in a case of IP-III.

Fig. 47

part. Then a thin layer of fascia is added again and then a tiny amount of glue is added. This is continued until the opening around the electrode is properly closed and no CSF leakage is witnessed.

As a principle the surgeon should not leave the surgery without completely controlling the CSF leakage around the electrode. If there is a severe gusher postoperative continuous lumbar drainage may divert the CSF away from the cochleostomy area allowing the healing of the cochleostomy area. This is kept in place for 4–5 days. In case of difficult control of CSF gusher subtotal petrosectomy can be an additional precaution to eliminate the connection between the nasopharynx and the middle ear to prevent meningitis. However it should never be forgotten that subtotal petrosectomy is an additional measure and the first line of defense of proper control of the cochleostomy is mandatory.

B-Misplacement into the IAC:

Because of the wide connection between the IAC and the cochlea the electrode may go into the IAC inadvertently. Intraoperative radiology is advisable to check the position of the electrode. Modiolar hugging electrodes tend to turn towards the center of the cochlea where the defect is greatest. These type electrodes may go into the IAC more than the straight ones. If the postoperative X-ray shows a straight electrode revision should be planned as soon as possible.

Conclusion

IP-III is the rarest form of inner ear malformations and is observed in X-linked deafness. Because of the conductive component a stapedectomy is usually planned. In patients with congenital hearing loss a HRCT will demonstrate this pathology and a stapedectomy which may result in further hearing loss can be avoided. Hearing aid or cochlear implant can be offered according to the degree of hearing loss. In CI surgery a gusher and misplacement into the IAC may complicate the surgery. Every effort should be shown to fully control the CSF leakage.

References

1 Nance WE, Setleff R, McLeod A, Sweeney A, Cooper C, McConnell F: X-linked mixed deafness with congenital fixation of the stapedial footplate and perilymphatic gusher. Birth Defects Orig Artic Ser [Research Support, U.S. Gov't, Non-P.H.S.] 1971;7:64–69.

2 Papadaki E, Prassopoulos P, Bizakis J, Karampekios S, Papadakis H, Gourtsoyiannis N: X-linked deafness with stapes gusher in females. Eur J Radiol [Case Reports] 1998;29:71–75.

3 Bento RF, Miniti A: X-linked mixed hearing loss: four case studies. The Laryngoscope 1985;95:462–468.

4 Kumar G, Castillo M, Buchman CA: X-linked stapes gusher: CT findings in one patient. AJNR American journal of neuroradiology [Case Reports] 2003;24:1130–1132.

5 Talbot JM, Wilson DF: Computed tomographic diagnosis of X-linked congenital mixed deafness, fixation of the stapedial footplate, and perilymphatic gusher. The American journal of otology [Case Reports Comparative Study] 1994;15:177–182.

6 de Kok YJ, van der Maarel SM, Bitner-Glindzicz M, Huber I, Monaco AP, Malcolm S, et al: Association between X-linked mixed deafness and mutations in the POU domain gene POU3F4. Science [Research Support, Non-U.S. Gov't] 1995;267:685–688.

7 Phelps PD, Reardon W, Pembrey M, Bellman S, Luxom L: X-linked deafness, stapes gushers and a distinctive defect of the inner ear. Neuroradiology 1991;33:326–330.

8 Snik AF, Hombergen GC, Mylanus EA, Cremers CW: Air-bone gap in patients with X-linked stapes gusher syndrome. The American journal of otology [Case Reports] 1995;16:241–246.

9 Tang A, Parnes LS: X-linked progressive mixed hearing loss: computed tomography findings. Ann Otol Rhinol Laryngol [Case Reports] 1994;103:655–657.

10 Sennaroglu L, Sarac S, Ergin T: Surgical results of cochlear implantation in malformed cochlea. Otology & neurotology : official publication of the American Otological Society, American Neurotology Society [and] European Academy of Otology and Neurotology [Case Reports] 2006;27:615–623.

11 Chee NW, Suhailee S, Goh J: Clinics in diagnostic imaging (111): X-linked congenital mixed deafness syndrome. Singapore Med J 2006;47:822–824; quiz 5.

12 Sennaroglu L: Cochlear implantation in inner ear malformations —a review article. Cochlear implants international 2009 Apr 8.

4 Internal Auditory Canal

IAC Stenosis

The morphology (diameter and length) of the internal auditory canal (IAC) has previously been described based on measurements either of the temporal bone itself or using tomography, but recently many reports are emerging based on measurements taken using high-resolution CT images. Among these, a report by McClay et al [1] divides test subjects into two groups based on presence or absence of sensorineural hearing loss and measures and examines a large number of samples of IAC morphology. The results show that the IAC's anteroposterior diameter (as measured in an axial image, 2 mm lateral to the medial margin of the IAC's posterior wall) was 5.02 ± 1.22 mm in the group with no sensorineural hearing loss (307 samples) and 4.85 ± 1.07 mm in the group with sensorineural hearing loss (181 samples), with no significant difference between the two. Even the superoinferior diameter (as measured at the point of maximum vertical breadth at the IAC's midpoint) was 4.62 ± 1.16 mm in the group with no sensorineural hearing loss (292 samples) and 4.39 ± 1.18 mm in the group with sensorineural hearing loss (175 samples), again with no significant difference between the two. Consequently, it is difficult to determine a normal range for IAC diameter based simply on presence or absence of hearing loss alone. IAC length was also about the same in both groups, at around 11 mm. However, on examination of samples accompanied by malformation of the inner ear, one finds many cases of sensorineural hearing loss in which anteroposterior or superoinferior IAC diameter is 2 mm or less. On the other hand, enlargement of the internal auditory canal (defined in McClay's paper as an anteroposterior or superoinferior diameter of 8 mm or greater) is unrelated to hearing loss.

According to Lang's measurements [2], IAC diameter in newborns is approx. 3 mm, and approx. 4.5 mm in two years old, whereas in adults is it 6–7 mm, suggesting that it expands with age. The internal auditory canal also lengthens from around 5–7 mm at birth to 10–15 mm in adulthood. However, according to measurements using 3-dimensional computer reconstructions based on temporal bone histopathological samples by Sakashita and Sando [3], while the internal auditory canal clearly does grow longer, its increase in diameter with age is minimal or, at most, very slight. For example, if we measure the internal auditory canals in the pediatric standard temporal bone CT images at four months, one year, three years, and 16 years shown in this book according to McClay's method described above, IAC length increases with age, with a length of 5.8 mm at four months, 7.7 mm at one year, 10.6 mm at three years, and 12.9 mm at 16 years. The anteroposterior diameters, on the other hand, are 3.5 mm, 3.8 mm, 6.7 mm, and 4.8 mm respectively, indicating a somewhat narrower diameter in early years, although the individual differences are considerable, and it lacks the same clear enlargement trend seen with length. Consequently, the pattern of development for the internal auditory canal can be understood as one of lengthening with almost no change in diameter.

Development of the internal auditory canal is related to the formation and development of cranial nerve VIII, and cranial nerve VIII hypoplasty is accompanied by aplasia and stenosis of the internal auditory canal [4]. The indication of cochlear implants must be considered in cases of profound bilateral hearing loss, and the presence of IAC stenosis is an important factor to consider at this time. Generally, the success rate of cochlear implants in cases of IAC stenosis is lower than in those in which stenosis is not a factor [5].

On the other hand, the condition of the facial nerve, another nerve which traverses the internal auditory canal, does not necessarily correlate to IAC diameter, and even in the following cases containing IAC stenosis with cranial nerve VIII hypoplasia, there are no facial nerve abnormalities.

References

1 McClay JE, Tandy R, Grundfast K, et al: Major and minor temporal bone abnormalities in children with and without congenital sensorineural hearing loss. Arch Otolaryngol Head Neck Surg 2002; 128:664–671.

2 Lang J: Neuroanatomie der Nn. Opticus, Trigeminus, Facialis, Glossopharyngeus, Vagus, Accessorius und Hypoglossus. Arch Otorhinolaryngol 1981;231:1–69.

3 Sakashita T, Sando I: Postnatal development of the internal auditory canal studied by computer-aided three-dimansional reconstruction and measurement. Ann Otol Rhinol Laryngol 1995;104:469–475.

4 McPhee JR, Van de Water TR: Epithelial-mesenchymal tissue interactions guiding otic capsule formation: the role of the otocyst. J Embryol Exp Morphol 1986; 97:1–24.

5 Papsin BC: Cochlear implantation in children with anomalous cochleovestibular anatomy. Laryngoscope 2005; 115 (Suppl. 106):1–26.

Case 1

IAC Stenosis

Subject: female, 5 years old

History and Clinical Findings

The subject had been healthy since birth and her parents were not aware of any particular problems, but recently when her parents held the phone up to her right ear she said she couldn't hear anything so they became worried and took her to the doctor. Pure tone audiometry (fig. 48) indicated average hearing level of 93.3 dB right and 13.3 dB left, for a finding of unilateral profound hearing loss in the right ear. For objective audiometry, ASSR testing was carried out, with right ear thresholds of from 100 dB (500 Hz) to 110 dB scale-out (4,000 Hz), whereas left ear thresholds were all less than 20 dB from 500 Hz to 4,000 Hz, confirming the finding of unilateral deafness in the right ear (fig. 49). In DPOAE testing as well, the right ear showed no response, while in the left ear response was normal. Temporal bone CT and MRI exams were conducted to further determine the cause. Image findings for the subject's affected (right) and healthy (left) ears are shown below.

Patient CT Findings

No abnormalities were found in the middle ear or ossicles in either side. In the inner ear as well, no clear morphological abnormalities were discovered in the cochlea or vestibule. However, the right internal auditory canal is clearly narrower, with an anteroposterior diameter at the opening to the posterior cranial fossa of 3.5 mm, just 60% the size of the healthy left side diameter of 5.7 mm (fig. 50:3R, 3L). Observing the lateral end of the internal auditory canal at its border with the modiolus, diameter of the opening at the base of the modiolus is less than 1 mm on the affected side, compared to 2.7 mm on the healthy side (fig. 50:1R, 1L). On the other hand, the facial nerve shows no bilateral discrepancies in either its path or thickness in the labyrinthine segment (fig. 50:2R, 2L). The singular foramen (through which the posterior ampullary nerve passes) on the affected side is more medial than normal and is separated from the internal auditory canal as it approaches the posterior ampulla (fig. 50:2R).

Examining the coronal images, there is a thin, tubular structure between the modiolus and the fundus of the internal auditory canal (fig. 51:1). This tunnel-like structure is not normally present (fig. 51:n1).

Patient MRI Findings

Almost no differences can be ascertained in cochlea itself between the affected and the healthy side, but the modiolus is somewhat narrower on the affected (right) side. In particular, the part corresponding to the cochlear area of the fundus of the internal auditory canal is clearly

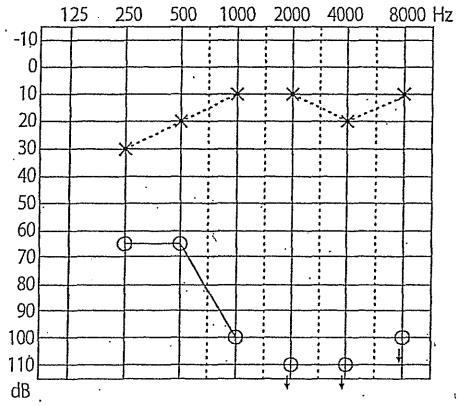

Fig. 48. (Case 1) Audiogram

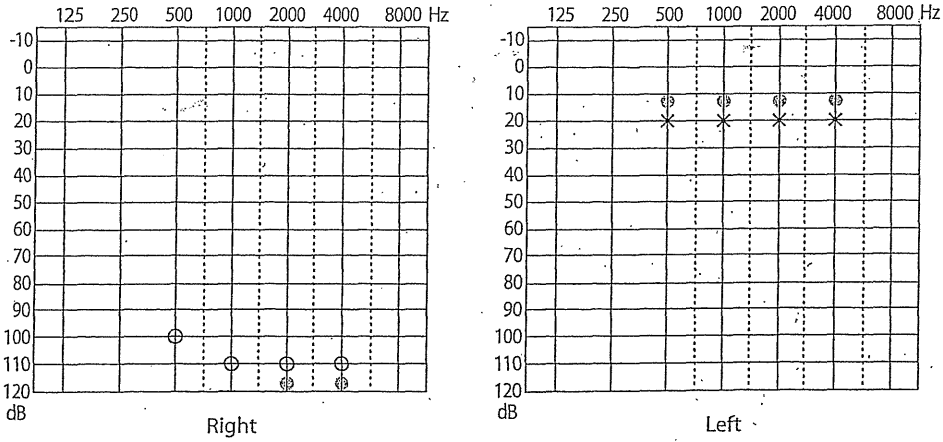

Fig. 49. (Case 1) ASSR test

Patient CT Findings

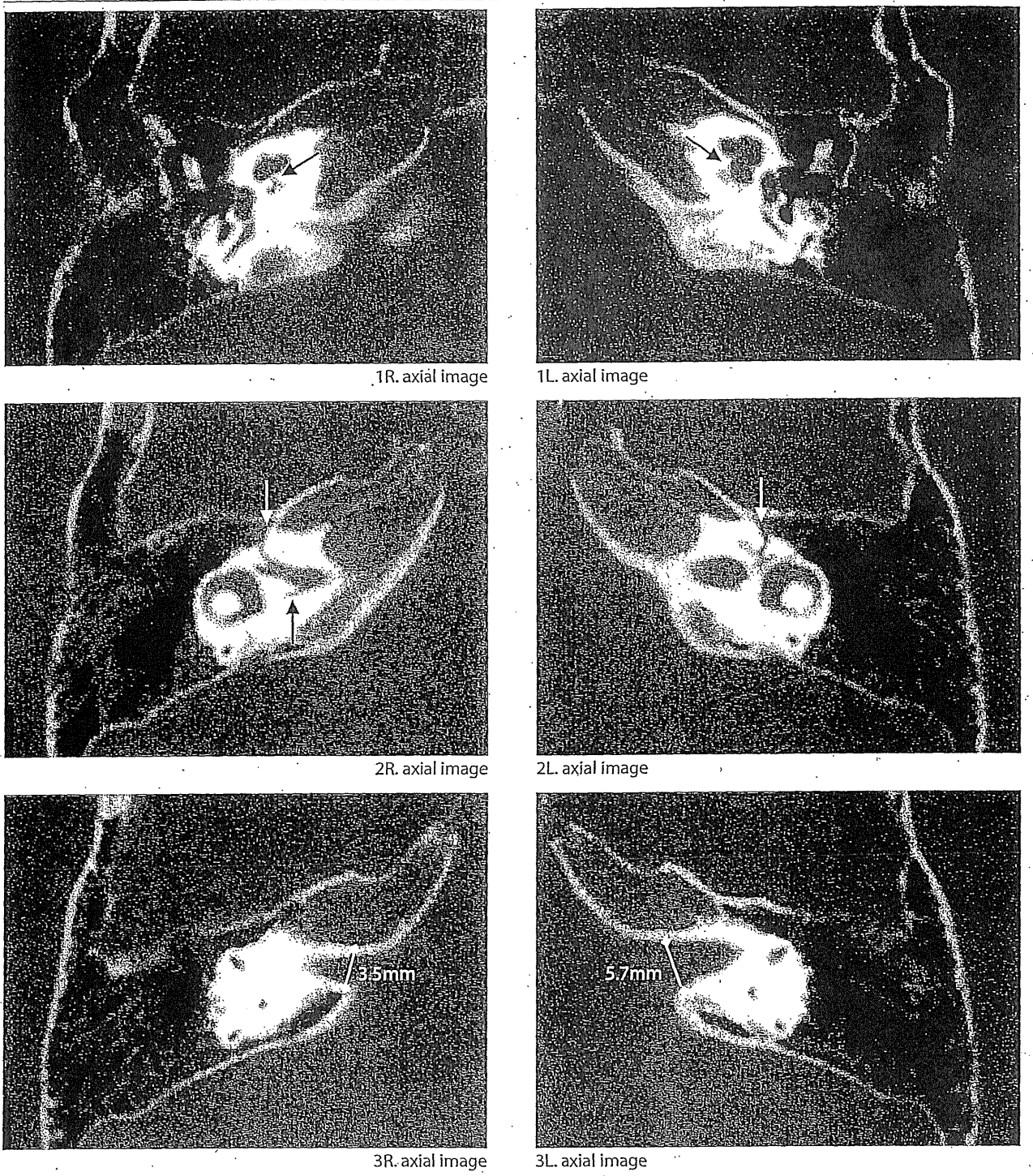

1R. axial image
1L. axial image
2R. axial image
2L. axial image
3R. axial image
3L. axial image

Fig. 50. (Case 1) CT: R=affected side, L=healthy side

[Patient CT Findings]

No abnormalities were found in the middle ear or ossicles in either side. In the inner ear as well, no clear morphological abnormalities were discovered in the cochlea or vestibule. However, the right internal auditory canal is clearly narrower, with an anteroposterior diameter at the opening to the posterior cranial fossa of 3.5 mm, just 60% the size of the healthy left side diameter of 5.7 mm (3R, 3L). Observing the lateral end of the internal auditory canal at its border with the modiolus, the diameter of the opening at the base of the modiolus is less than 1 mm on the affected side, compared to 2.7 mm on the healthy side (1R : ↙ ; 1L: ↘). On the other hand, the facial nerve shows no bilateral discrepancies in either its path or thickness in the labyrinthine segment (2R & 2L: ⇕). The singular foramen (through which the posterior ampullary nerve passes) on the affected side is more medial than normal and is separated from the internal auditory canal as it approaches the posterior ampulla (2R: ↑).

Patient CT Findings

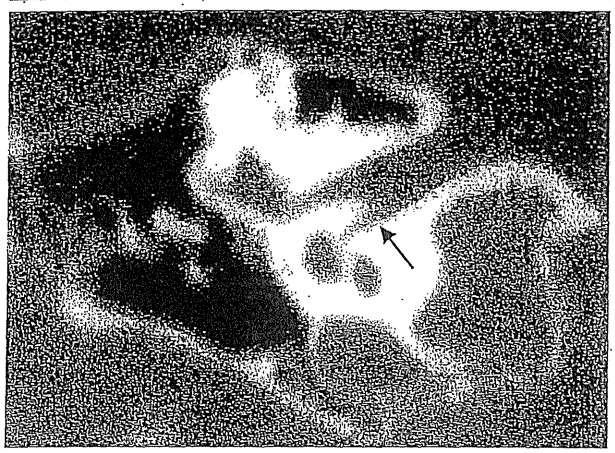

1. coronal image

Normal Control CT Findings

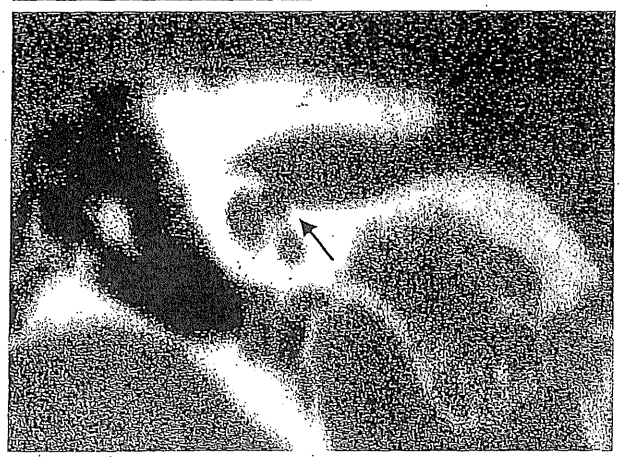

n1. coronal image

Fig. 51: (Case 1) CT

[Patient CT Findings]
There is a thin, tubular structure between the modiolus and the fundus of the internal auditory canal (1: ↖).

《Normal Control CT Findings》
Normally the base of the modiolus continues broadly into the internal auditory canal (n1: ↖).

narrower on the affected side than the healthy side, and the cochlear nerve, which is plainly visible in the healthy side, cannot be ascertained on the affected side (fig. 52:1R, 1L). Normally, cranial nerve VIII can be observed bifurcating into the cochlear nerve (fig. 52:2L) and the vestibular nerve slightly medial to the fundus of the internal auditory canal, but in this case the narrowness of the internal auditory canal prevents observation of this bifurcation (fig. 52:2R). Cranial nerves VII and VIII are visible at the cerebellopontine angle. On the affected right side, both nerves are straddling the two slices (fig. 52:3R-a, b), but on careful comparison of the two, cranial nerve VIII on the affected side appears thinner than on the healthy side, even in cross-section b where it is easier to see. On the other hand, cranial nerve VII does not display the same bilateral disparity. From the above findings, one can surmise that in this case there is hypoplasia or atrophy of the cochlear nerve and cranial nerve VIII.

Post-diagnostic Course

As a case of unilateral profound hearing loss, it is not essentially indicated for treatment using a hearing aid or cochlear implant. The decision was made to periodically check to ensure that no problems with hearing arose on the healthy side.

Points

1. Congenital IAC stenosis frequently accompanies sensorineural hearing loss, but enlargement does not correlate with hearing loss.
2. The length of the internal auditory canal increases after birth, but its diameter shows little change.
3. Internal auditory canal development is related to formation and development of cranial nerve VIII.
4. The success rate of cochlear implants in cases of IAC stenosis is lower than in those in which stenosis is not a factor.

Patient MRI Findings

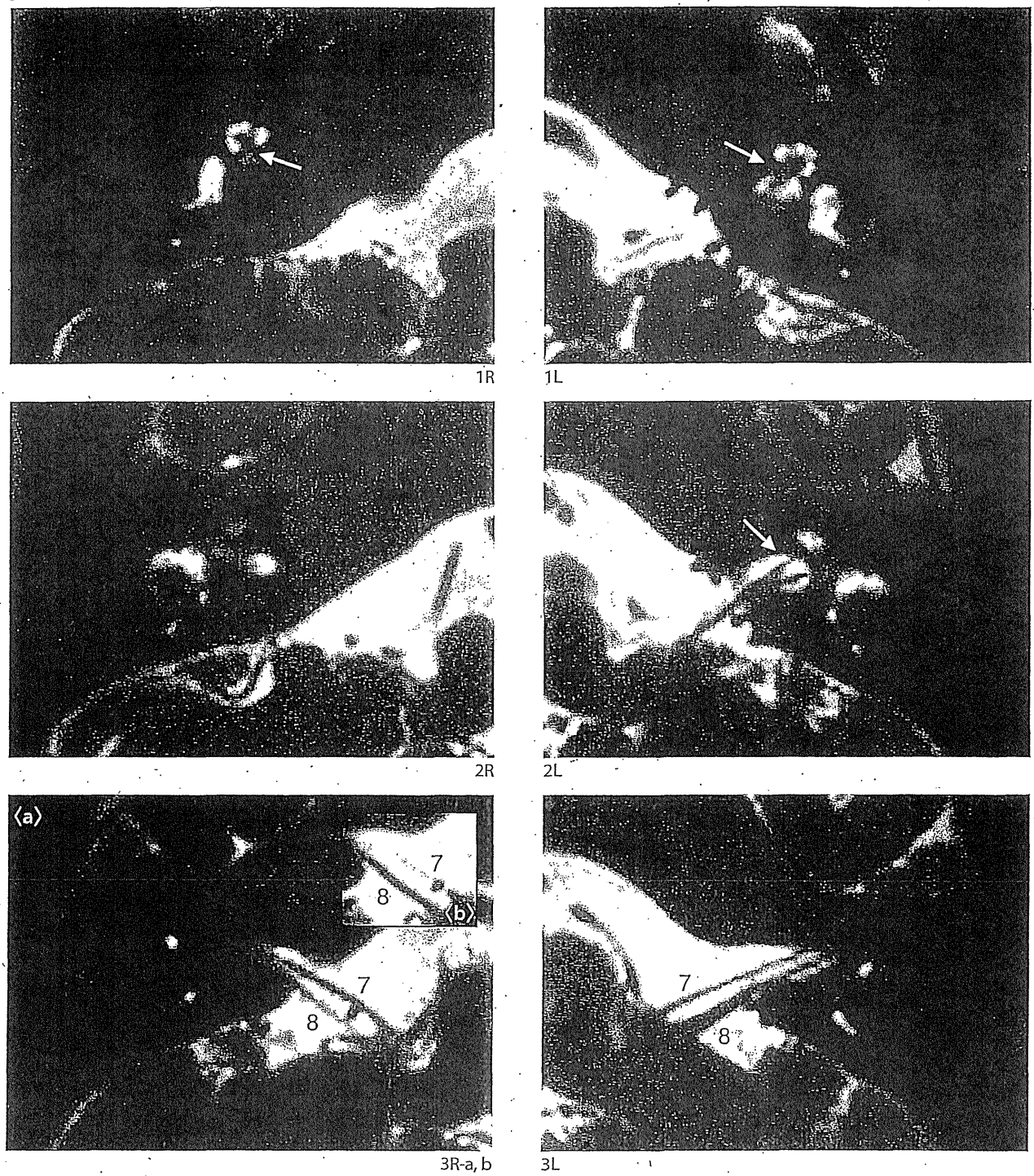

Fig. 52. (Case 1) MRI: R=affected side, L=healthy side

[Patient MRI Findings]

Almost no differences can be ascertained in cochlea itself between the affected and the healthy side, but the modiolus is somewhat narrower on the affected (right) side. In particular, the part corresponding to the cochlear area of the fundus of the internal auditory canal is clearly narrower on the affected side than the healthy side, and the cochlear nerve, which is plainly visible in the healthy side, cannot be ascertained on the affected side (1R: ; 1L:). Normally, cranial nerve VIII can be observed bifurcating into the cochlear nerve (2L:) and the vestibular nerve slightly medial to the fundus of the internal auditory canal, but in this case the narrowness of the internal auditory canal prevents observation of this bifurcation (2R). Cranial nerves VII and VIII can be observed at the cerebellopontine angle. On the affected right side, both nerves are straddling the two slices (3R-a, b), but on careful comparison of the two, cranial nerve VIII on the affected side is thinner than on the healthy side, even in cross-section b where it is easier to see. On the other hand, cranial nerve VII does not display the same bilateral disparity.

Case 2

Stenosis of Cochlear Nerve Canal

Subject: male, 1 year old

History and Clinical Findings

Four months previously (at eight months old), the subject was hospitalized at a pediatric hospital for bacterial meningitis. The meningitis was cured using antibiotics and steroid therapy but, when auditory brainstem response (ABR) testing was conducted before discharge from the hospital to check for inner ear dysfunction, no response was obtained in the right ear (fig. 53). The subject then was referred to our department for further testing.

ASSR testing conducted by our department returned near normal results for the left ear, but threshold values for the right ear were from 70 dB (500 Hz) to 110 dB (4,000 Hz) (fig. 54). However, DPOAE testing confirmed near normal response not only in the left ear, but in the right ear as well (fig. 55).

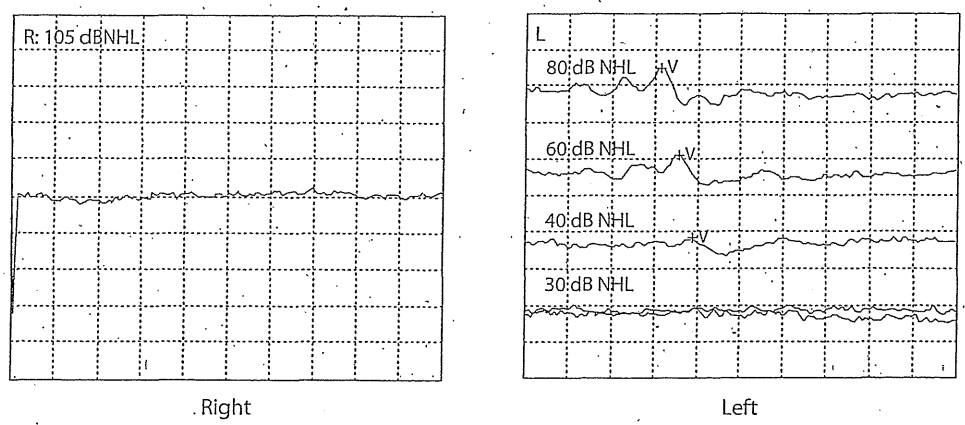

Fig. 53. (Case 2) Auditory brainstem response test (ABR)

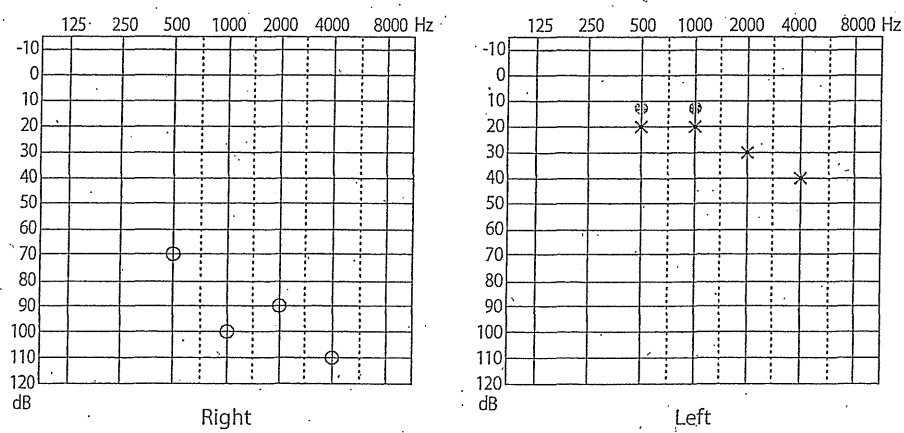

Fig. 54. (Case 2) ASSR test

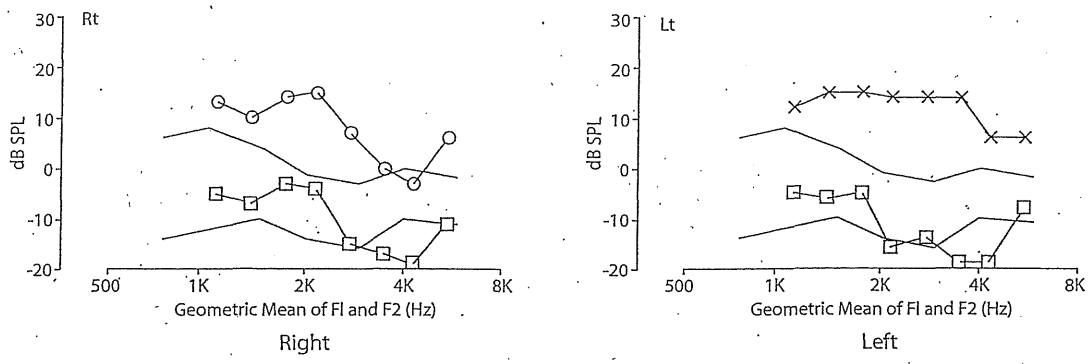

Fig. 55. (Case 2) DPOAE test